Multilevel Optimized Schwarz Methods Without Overlap for Highly Heterogeneous Media

Yvon Maday* Frédéric Magoulès†

25 March 2005

*Laboratoire Jacques-Louis Lions, Université Pierre et Marie Curie, BP 187, 75252 Paris Cedex 05, France, maday@ann.jussieu.fr, Division of Applied Mathematics, Brown University, 128 George Street, Providence RI 02912, USA

†Institut Elie Cartan de Nancy, Université Henri Poincaré, BP 239, 54506 Vandoeuvre-les-Nancy Cedex, France, frederic.magoules@iecn.u-nancy.fr

Abstract

In this paper an original variant of the Schwarz domain decomposition method is introduced for heterogeneous media. This method uses new optimized 'absorbing' interface conditions specially designed to take into account the heterogeneity between the sub-domains on each sides of the interfaces. Numerical experiments illustrate the dependency of the proposed method upon several parameters, and confirm the robustness and efficiency of this method based on such 'absorbing' interface conditions. Several mesh partitions taking into account multiple cross points are considered in these experiments.

Keywords

heterogeneous media, domain decomposition method, Schwarz algorithm, 'absorbing' interface condition, coarse space correction

Résumé

Dans ce papier, une variante originale de la méthode de Schwarz est introduite pour traiter le cas de milieux hétérogènes. Cette méthode utilise de nouvelles conditions d'interfaces dites 'absorbantes' spécialement conçues pour tenir compte de l'hétérogénéité du milieu entre les sous-domaines. Des expériences numériques illustrent la dépendance de la méthode proposée en fonction de nombreux paramètres, et confirment la robustesse et l'efficacité de cette méthode basée sur de telles conditions d'interfaces. Plusieurs configurations de découpage en sous-domaines, faisant notamment apparaître des coins, sont considérées dans ces expériences.

Mots clefs

milieu hétérogène, méthode de décomposition de domaine, algorithme de Schwarz, conditions d'interfaces 'absorbantes', espace grossier

1 Introduction

The classical Schwarz algorithm [1, 2] has a long history. Several variants of this algorithm have been developed and analyzed these last twenty years [3, 4, 5]. Both overlapping and non-overlapping Schwarz algorithms have been designed [6, 7, 8] for a wide range of equations. Several preconditioning techniques have been investigated, as interface conditions [9, 10, 11], Aitken like methods [12, 13, 14], coarse space correction [15, 16, 17, 18, 19, 20]. Recent areas of interests concern the improvement of these methods for highly heterogeneous media [21, 22, 23].

The interface conditions of the Schwarz algorithm without overlap have a strong influence on the convergence of the algorithm. Optimal interface conditions which lead to the best possible convergence of the Schwarz algorithm can be derived, and are linked with the Steklov-Poincaré operator [24, 25, 26]. These optimal interface conditions however are non-local in nature and several works continue to be investigated in order to use them efficiently in numerical simulations [27]. Other approaches consist in approximating these optimal interface conditions with local operators. These local operators could then be optimized for performance of the Schwarz algorithm, similar to the previous works performed on other equations [24, 28, 25, 26]. When dealing with heterogeneous media, the heterogeneity of the media between two subdomains requires a special treatment. For this purpose, several techniques to design efficient and original interface conditions are here investigated.

The structure of this paper is the following. Section 2 presents the analysis of the Schwarz algorithm with 'absorbing' interface conditions in the Fourier space. The optimal convergence property of this algorithm is presented, and the optimal interface conditions are derived. Section 3 presents three techniques to design efficient approximations of these optimal interface conditions. These techniques are based on the optimization of the convergence rate of the Schwarz algorithm. An original and rigorous theoretical analysis of the associated optimization problem is performed. Two of these techniques are specially designed to take into account the heterogeneity of the media on the interfaces, and lead to impressive convergence results. Section 4 presents the discretization and the linear system condensed on the interface. This linear system is solved iteratively with a Krylov method. Section 5 introduces an additional coarse space correction in this iterative method to take into account the dependancy in the number of sub-domains. Section 6 shows some numerical experiments and illustrates the convergence of the Schwarz algorithm equipped

with these new interface conditions. Even though all the optimizations are performed on a model problem in the whole plane, the derived optimized interface conditions can be used for general decompositions, as illustrated in the numerical experiments. The case of cross-points i.e. points where more than two sub-domains intersect, is presented too. Finally, in Section 7 the conclusion of this paper is presented.

2 The Schwarz Method with 'Absorbing' Interface Conditions

The following equation in an heterogenous media is considered

$$(-\nabla \cdot (\mu \nabla))\, u(x,y) = f(x,y), \quad x,y \in \Omega$$

in the domain $\Omega = \mathbb{R}^2$ with the condition at infinity,

$$\lim_{r\to\infty} u = 0,$$

where $r = \sqrt{x^2+y^2}$ and $\mu \in \mathbb{R}^+$. The domain Ω is decomposed into two non-overlapping sub-domains $\Omega^{(1)} = (-\infty, 0] \times \mathbb{R}$ and $\Omega^{(2)} = [0, \infty) \times \mathbb{R}$. The Schwarz algorithm with 'absorbing' interface condition reads

$$\begin{cases} \left(-\nabla \cdot (\mu^{(1)} \nabla)\right) u_{n+1}^{(1)}(x,y) = f(x,y), \quad x,y \in \Omega^{(1)} & (2.1) \\ \left(\mu^{(1)}\partial_x + \mathcal{A}^{(1)}\right) u_{n+1}^{(1)}(0,y) = \left(\mu^{(2)}\partial_x + \mathcal{A}^{(1)}\right) u_n^{(2)}(0,y) & (2.2) \end{cases}$$

$$\begin{cases} \left(-\nabla \cdot (\mu^{(2)} \nabla)\right) u_{n+1}^{(2)}(x,y) = f(x,y), \quad x,y \in \Omega^{(2)} & (2.3) \\ \left(\mu^{(2)}\partial_x + \mathcal{A}^{(2)}\right) u_{n+1}^{(2)}(0,y) = \left(\mu^{(1)}\partial_x + \mathcal{A}^{(2)}\right) u_n^{(1)}(0,y) & (2.4) \end{cases}$$

where n represents the iteration parameter. The operators $\mathcal{A}^{(1)}$ and $\mathcal{A}^{(2)}$ are to be determined for the best performance of the algorithm. They are obtained in order to minimize the convergence rate of the algorithm.

To analyze the convergence, it suffices to consider by linearity the case of $f(x,y) = 0$ and to analyze the convergence to zero. For this purpose the Fourier transform is used in the y direction defined for a function g by

$$\hat{g}(x,k) = \int_{-\infty}^{+\infty} e^{-iky}\, g(x,y)\, dy$$

and applied to the systems of equations (2.1) to (2.4). For simplicity the coefficient μ is assumed to be constant per sub-domains. In this case the following is obtained:

$$\begin{cases} \left(-\mu^{(1)}\partial_{xx}^2 + \mu^{(1)}k^2\right)\hat{u}_{n+1}^{(1)}(x,k) = 0, \quad x < 0,\ k \in \mathbb{R} & (2.5) \\ \left(\mu^{(1)}\partial_x + \Theta^{(1)}\right)\hat{u}_{n+1}^{(1)}(0,k) = \left(\mu^{(2)}\partial_x + \Theta^{(1)}\right)\hat{u}_n^{(2)}(0,k) & (2.6) \end{cases}$$

$$\begin{cases} \left(-\mu^{(2)}\partial_{xx}^2 + \mu^{(2)}k^2\right)\hat{u}_{n+1}^{(2)}(x,k) = 0, \quad x > 0,\ k \in \mathbb{R} & (2.7) \\ \left(\mu^{(2)}\partial_x + \Theta^{(2)}\right)\hat{u}_{n+1}^{(2)}(0,k) = \left(\mu^{(1)}\partial_x + \Theta^{(2)}\right)\hat{u}_n^{(1)}(0,k) & (2.8) \end{cases}$$

where $\Theta^{(s)}(k),\ s = 1,2$ denotes the symbol of operator $\mathcal{A}^{(s)}$ and k is the Fourier variable, also called frequency. The general solution of these ordinary differential equations is

$$\hat{u}_{n+1}^{(s)}(x,k) = A^{(s)}\ e^{\Lambda^{(s)}(k)\ x} + B^{(s)}\ e^{-\Lambda^{(s)}(k)\ x}, \quad s = 1,2$$

where $\Lambda^{(s)}(k) = |k|$, denotes the root of the characteristic equation

$$-\mu^{(s)}(\Lambda^{(s)}(k))^2 + \mu^{(s)}k^2 = 0.$$

Taking into account the condition at infinity, the solutions are

$$\begin{aligned} \hat{u}_{n+1}^{(1)}(x,k) &= \hat{u}_{n+1}^{(1)}(0,k)\ e^{\Lambda^{(1)}(k)\ x} \\ \hat{u}_{n+1}^{(2)}(x,k) &= \hat{u}_{n+1}^{(2)}(0,k)\ e^{-\Lambda^{(2)}(k)\ x}. \end{aligned}$$

Using the interface conditions and the fact that

$$\begin{aligned} \partial_x\hat{u}_{n+1}^{(1)}(x,k) &= \Lambda^{(1)}(k)\ \hat{u}_{n+1}^{(1)}(x,k) \\ \partial_x\hat{u}_{n+1}^{(2)}(x,k) &= -\Lambda^{(2)}(k)\ \hat{u}_{n+1}^{(2)}(x,k) \end{aligned}$$

the following is obtained

$$\begin{aligned} \hat{u}_{n+1}^{(1)}(x,k) &= \hat{u}_n^{(2)}(0,k)\ \frac{-\mu^{(2)}\Lambda^{(2)}(k) + \Theta^{(1)}(k)}{\mu^{(1)}\Lambda^{(1)}(k) + \Theta^{(1)}(k)}\ e^{\Lambda^{(1)}(k)\ x} \\ \hat{u}_{n+1}^{(2)}(x,k) &= \hat{u}_n^{(1)}(0,k)\ \frac{\mu^{(1)}\Lambda^{(1)}(k) + \Theta^{(2)}(k)}{-\mu^{(2)}\Lambda^{(2)}(k) + \Theta^{(2)}(k)}\ e^{-\Lambda^{(2)}(k)\ x}, \end{aligned}$$

where $\Theta^{(1)}(k)$ and $\Theta^{(2)}(k)$ are assumed to be with real value. Evaluating the second equation at $x = 0$ for iteration n and inserting it into the first equation, the following can be stated after evaluating it again at $x = 0$

$$\hat{u}^{(1)}_{n+1}(0,k) = \hat{u}^{(1)}_{n-1}(0,k)\ \frac{-\mu^{(2)}\Lambda^{(2)}(k) + \Theta^{(1)}(k)}{\mu^{(1)}\Lambda^{(1)}(k) + \Theta^{(1)}(k)}\ \frac{\mu^{(1)}\Lambda^{(1)}(k) + \Theta^{(2)}(k)}{-\mu^{(2)}\Lambda^{(2)}(k) + \Theta^{(2)}(k)}.$$

Defining the convergence rate $\kappa(k)$ by

$$\kappa(k) = \frac{\mu^{(2)}\Lambda^{(2)}(k) - \Theta^{(1)}(k)}{\mu^{(1)}\Lambda^{(1)}(k) + \Theta^{(1)}(k)}\ \frac{\mu^{(1)}\Lambda^{(1)}(k) + \Theta^{(2)}(k)}{\mu^{(2)}\Lambda^{(2)}(k) - \Theta^{(2)}(k)}. \tag{2.9}$$

it can be found by induction that

$$\hat{u}^{(1)}_{n+1}(0,k) = \kappa(k)\ \hat{u}^{(1)}_{n-1}(0,k),$$

and by a similar calculation on the second sub-domain

$$\hat{u}^{(2)}_{n+1}(0,k) = \kappa(k)\ \hat{u}^{(2)}_{n-1}(0,k).$$

The selection of the most appropriate operators $\Theta^{(1)}$ and $\Theta^{(2)}$ is now given by the following theorem.

Theorem 2.1 (Optimal 'Absorbing' Interface Conditions) *With the following selection*

$$\Theta^{(1)}(k) = \mu^{(2)}\Lambda^{(2)}(k), \quad \Theta^{(2)}(k) = -\mu^{(1)}\Lambda^{(1)}(k)$$

the Schwarz algorithm defined by equations (2.5)-(2.8) converges in two iterations.

Proof 2.1 *Substitution of $\Theta^{(1)}(k) = \mu^{(2)}\Lambda^{(2)}(k)$ and $\Theta^{(2)}(k) = -\mu^{(1)}\Lambda^{(1)}(k)$ in the expression of the convergence rate (2.9), leads to $\kappa(k) = 0$ and the algorithm converges in two steps independently of the initial estimate.*

This optimal selection of the operators $\Theta^{(1)}$ and $\Theta^{(2)}$ in the Fourier space, leads to the convergence of the algorithm in two iterations. This choice corresponds to $\mathcal{A}^{(1)}$ and $\mathcal{A}^{(2)}$ in the physical space, equal to Steklov-Poincaré operators. Such operators are non-local by definition. Several research have been carried out these last ten years in order to use efficiently such operators in numerical simulation [27]. Other approaches consist of building local approximation of these optimal operators, as done in the previous works [24, 28, 25, 26] for other equations.

3 Optimized 'Absorbing' Interface Conditions

In this section, the non-local optimal operators, involving the symbol $|k|$ in the Fourier space, are approximated by some constants, which represent differential operators in the physical space and are thus local.

Different techniques of approximation have been analyzed in the recent years for other equations. The first results presented in references [29, 30] for the Helmholtz equation, use a simple zero order Taylor expansion of the Steklov-Poincaré operator, i.e. $\Theta^{(s)}(k)$ is a constant independant of k. In reference [25] for the Euler equations, in reference [26] for the Maxwell equation, and in references [31, 28] for the Helmholtz equation, the constant is designed through an optimization procedure. They are selected in such a way that they minimize the convergence rate of the Schwarz algorithm. Later, more complex optimization procedures have been developed [26, 25, 24] based on second order Taylor expansion and involve polynomial expressions of degree two upon the variable k in the Fourier space, which represent tangential differential operators in the physical space.

Using these interface conditions in the Schwarz algorithm, can be interpreted [32] as a local preconditioning technique. Other preconditioning techniques, like the Aitken method [12, 13, 14], optimize the trace of the Fourier modes on the interface.

In the following sub-sections, the optimal operators are approximated by some constants in the Fourier space, which lead to Robin interface conditions in the physical space. Several approaches to define these Robin interface condition are investigated in the next sub-section.

3.1 One Parameter Based Robin Interface Conditions

The simplest approximation of the optimal operators consists in the following local operators:

$$\Theta^{(1)}(k) = \alpha, \quad \Theta^{(2)}(k) = -\alpha. \tag{3.1}$$

with $\alpha \in \mathbb{R}^+$. Inserting these approximations into the convergence rate gives

$$\kappa(\alpha, k) = \frac{\mu^{(2)}|k| - \alpha}{\mu^{(1)}|k| + \alpha} \frac{\mu^{(1)}|k| - \alpha}{\mu^{(2)}|k| + \alpha}. \tag{3.2}$$

Similar to the previous works for the Helmholtz equation [24, 31, 28], the optimal parameter α is obtained from the optimization problem:

$$\min_{\alpha \in \mathbb{R}^+} \left(\max_{k \in (k_{\min}, k_{\max})} |\kappa(\alpha, k)| \right) \tag{3.3}$$

where $k_{\min}$ denotes the smallest frequency relevant to the sub-domain and $k_{\max}$ denotes the largest frequency supported by the numerical grid. This largest frequency is of the order π/h for finite elements discretization. Due to the symmetry of the function $|\kappa(\alpha, k)|$ upon the variable k, only positive frequencies are considered in the optimization problem, i.e. $0 < k_{\min} \leq k \leq k_{\max}$. Several Lemmas are now introduced to analyze the optimization problem.

Lemma 3.1 *Under the assumptions*

$$1 \leq \mu^{(1)} < \mu^{(2)}, \quad \text{and} \quad 0 < k_{\min} < \widetilde{\alpha} < k_{\max},$$

and if $\widetilde{\alpha}$ is supposed to be known, the function $|\kappa(\widetilde{\alpha}, k)|$ defined for $k \in (k_{\min}, k_{\max})$, reaches its minimum at the frequencies $k^* = \frac{\widetilde{\alpha}}{\mu^{(1)}}$ and $k^* = \frac{\widetilde{\alpha}}{\mu^{(2)}}$.

Proof 3.1 *Substituting $\Theta^{(1)}$ and $\Theta^{(2)}$ given by (3.1) in the expression of the convergence rate (2.9) gives $\kappa(\widetilde{\alpha}, k)$. It is clear that $|\kappa(\widetilde{\alpha}, k)|$ vanishes only for the frequency $k^* = \frac{\widetilde{\alpha}}{\mu^{(1)}}$ and for the frequency $k^* = \frac{\widetilde{\alpha}}{\mu^{(2)}}$. Because the function $|\kappa(\widetilde{\alpha}, k)|$ takes positive value only, these two frequencies are obviously the frequencies where the function reaches its minimum.*

Lemma 3.2 *Under the assumptions*

$$1 \leq \mu^{(1)} < \mu^{(2)}, \quad \text{and} \quad 0 < k_{\min} < \widetilde{\alpha} < k_{\max}, \tag{3.4}$$

and if $\widetilde{\alpha}$ is supposed to be known, the function $|\kappa(\widetilde{\alpha}, k)|$ defined for $k \in (k_{\min}, k_{\max})$ reaches its maximum either at the frequency $k^* = k_{\min}$, $k^* = \frac{\widetilde{\alpha}}{\sqrt{\mu^{(1)}\mu^{(2)}}}$, or $k^* = k_{\max}$.

Proof 3.2 *The derivative of the function $|\kappa(\widetilde{\alpha}, k)|$ upon the variable k can be computed as:*

$$\kappa_k(\widetilde{\alpha}, k) = 2 sign\left(\frac{(\mu^{(2)}k - \widetilde{\alpha})(\mu^{(1)}k - \widetilde{\alpha})}{(\mu^{(1)}k + \widetilde{\alpha})(\mu^{(2)}k + \widetilde{\alpha})} \right) \frac{\widetilde{\alpha}(\mu^{(1)} + \mu^{(2)})(\mu^{(1)}\mu^{(2)}k^2 - \widetilde{\alpha}^2)}{(\mu^{(1)}k + \widetilde{\alpha})^2(\mu^{(2)}k + \widetilde{\alpha})^2}$$

where sign(.) denotes the sign function. This expression vanishes for $k^* = \frac{\widetilde{\alpha}}{\sqrt{\mu^{(1)}\mu^{(2)}}}$. *The sign of the function* $\kappa_k(\widetilde{\alpha}, k)$ *can then be analyzed as follows:*

$$\begin{cases} \kappa_k(\widetilde{\alpha}, k) < 0, \ \textit{for } k \in (k_{\min}, \dfrac{\widetilde{\alpha}}{\mu^{(2)}}) & (3.5) \\ \kappa_k(\widetilde{\alpha}, k) > 0, \ \textit{for } k \in (\dfrac{\widetilde{\alpha}}{\mu^{(2)}}, \dfrac{\widetilde{\alpha}}{\sqrt{\mu^{(1)}\mu^{(2)}}}) & (3.6) \\ \kappa_k(\widetilde{\alpha}, k) = 0, \ \textit{for } k = \dfrac{\widetilde{\alpha}}{\sqrt{\mu^{(1)}\mu^{(2)}}} & (3.7) \\ \kappa_k(\widetilde{\alpha}, k) < 0, \ \textit{for } k \in (\dfrac{\widetilde{\alpha}}{\sqrt{\mu^{(1)}\mu^{(2)}}}, \dfrac{\widetilde{\alpha}}{\mu^{(1)}}) & (3.8) \\ \kappa_k(\widetilde{\alpha}, k) > 0, \ \textit{for } k \in (\dfrac{\widetilde{\alpha}}{\mu^{(1)}}, k_{\max}). & (3.9) \end{cases}$$

From the previous analysis, and because $|\kappa(\widetilde{\alpha}, k)|$ *is a continuous function, the maximum is achieved at one of the frequencies* $k^* = k_{\min}$, $k^* = \frac{\widetilde{\alpha}}{\sqrt{\mu^{(1)}\mu^{(2)}}}$, *or* $k^* = k_{\max}$.

From Lemma 3.2, the maximum of the function $|\kappa(\alpha, k)|$ is reached at one of the following frequencies: $k_{\min}$, $\frac{\alpha}{\sqrt{\mu^{(1)}\mu^{(2)}}}$, or $k_{\max}$. The maximum is thus equal to one of the following values:

$$\begin{cases} |\kappa(\alpha, k_{\min})| = \left| \dfrac{\mu^{(2)}k_{\min} - \alpha}{\mu^{(1)}k_{\min} + \alpha} \ \dfrac{\mu^{(1)}k_{\min} - \alpha}{\mu^{(2)}k_{\min} + \alpha} \right| & (3.10) \\ |\kappa(\alpha, \dfrac{\alpha}{\sqrt{\mu^{(1)}\mu^{(2)}}})| = \left| \dfrac{(-\mu^{(2)} + \sqrt{\mu^{(1)}\mu^{(2)}})(-\mu^{(1)} + \sqrt{\mu^{(1)}\mu^{(2)}})|}{(\mu^{(1)} + \sqrt{\mu^{(1)}\mu^{(2)}})(\mu^{(2)} + \sqrt{\mu^{(1)}\mu^{(2)}})} \right| & (3.11) \\ |\kappa(\alpha, k_{\max})| = \left| \dfrac{\mu^{(2)}k_{\max} - \alpha}{\mu^{(1)}k_{\max} + \alpha} \ \dfrac{\mu^{(1)}k_{\max} - \alpha}{\mu^{(2)}k_{\max} + \alpha} \right|. & (3.12) \end{cases}$$

Under the assumptions of Lemma 3.2, the min-max problem reduces to:

$$\min_{\alpha \in (k_{\min}, k_{\max})} \left(\max \left(|\kappa(\alpha, k_{\min})|, \ |\kappa(\alpha, \frac{\alpha}{\sqrt{\mu^{(1)}\mu^{(2)}}})|, \ |\kappa(\alpha, k_{\max})| \right) \right)$$

which makes this optimization problem very easy to solve numerically. As illustrated in the following example with the parameters $h = 1/400$, $\mu^{(1)} = 1$

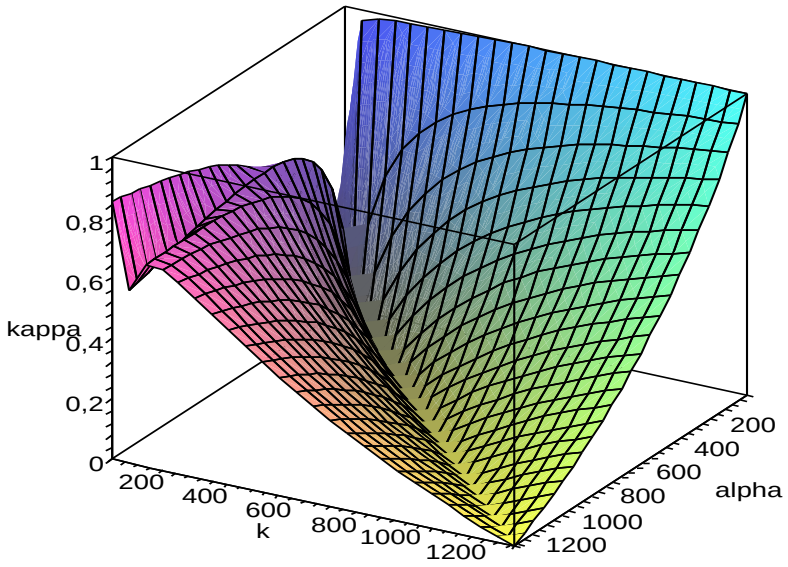

Figure 1: Convergence rate upon the frequency and the parameter to be optimized for $\Theta^{(1)} = -\Theta^{(2)} = \alpha$. ($h = 1/400$, $\mu^{(1)} = 1$, $\mu^{(2)} = 10^2$).

and $\mu^{(2)} = 10^2$, there may not be an unique solution to this min-max problem. The function $|\kappa(\alpha, k)|$ is represented upon the parameter α and the frequency k in the Figure 1. The maximum of the function $|\kappa(\alpha, k)|$ over the considered frequencies $(k_{\min}, k_{\max})$ is represented upon the parameter α in the Figure 2. As

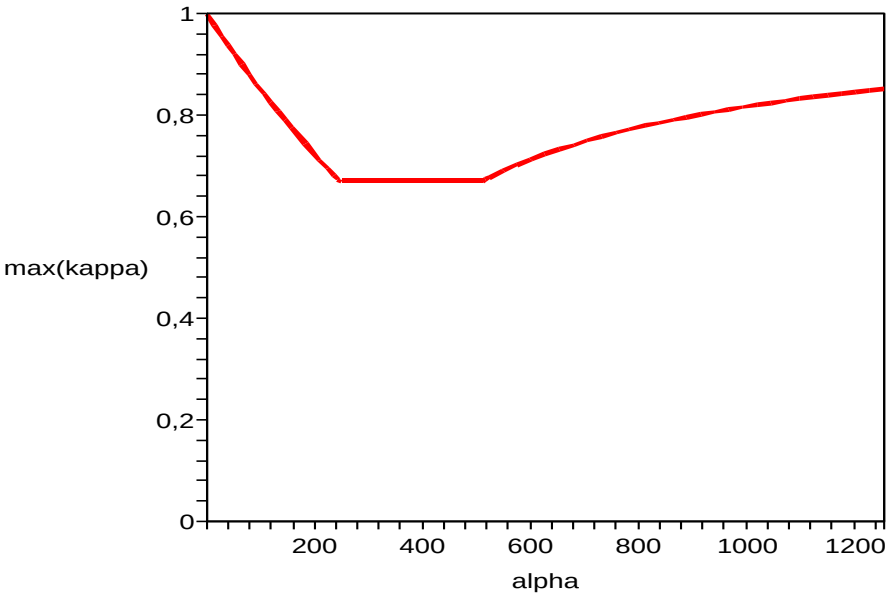

Figure 2: Maximum of the convergence rate upon the parameter to be optimized for $\Theta^{(1)} = -\Theta^{(2)} = \alpha$. ($h = 1/400$, $\mu^{(1)} = 1$, $\mu^{(2)} = 10^2$).

shown in this Figure there is not an unique solution to the optimization problem. This optimal parameter was found to be left bounded by $\alpha^* = 255.3527$ which gives an overall convergence rate $\kappa^* = 0.6693$. The optimized convergence rate associated to this optimal parameter is presented in the Figure 3.

Remark 3.1 *The analytic expression of one of the solution of the min-max problem is not straightforward and is still under current investigation. For this reason, a numerical optimization procedure will be performed in the numerical experiments section to find one optimal parameter.*

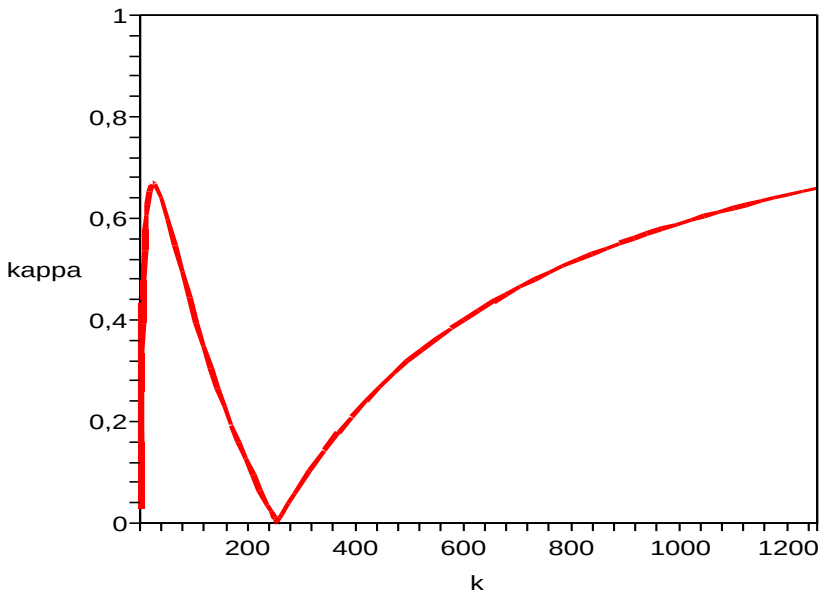

Figure 3: Optimized convergence rate upon the frequency for $\Theta^{(1)} = -\Theta^{(2)} = \alpha^*$. ($h = 1/400$, $\mu^{(1)} = 1$, $\mu^{(2)} = 10^2$).

3.2 One and Half Parameter Based Robin Interface Conditions

The expression of the optimal operators suggests to approximate these non-local operators in such a way that the property of the heterogeneity of the media remains in the expression of the local approximations. If a single constant is used to approximate these optimal operators, the following approximations

$$\Theta^{(1)}(k) = \mu^{(2)}\alpha, \quad \Theta^{(2)}(k) = -\mu^{(1)}\alpha, \tag{3.13}$$

with $\alpha \in \mathbb{R}^+$, reflects the heterogeneity of the media. In this case, how to choose the optimal parameter α is given by the following:

Theorem 3.1 (Optimized Robin Interface Conditions) *Under the assumptions*

$$0 < \mu^{(1)} < \mu^{(2)}, \quad \text{and} \quad 0 < k_{\min} < \alpha < k_{\max}, \tag{3.14}$$

the solution of the min-max problem (3.3) with $\Theta^{(1)}$ and $\Theta^{(2)}$ given by (3.13) rather than (3.1) is unique and the optimal parameter is given by

$$\alpha^* = \sqrt{k_{\min}k_{\max}}. \tag{3.15}$$

The optimized convergence rate (2.9) is then given by

$$\max_{k\in(k_{\min},k_{\max})} \kappa(\alpha^*,k) = \frac{\left(-\mu^{(2)}k_{\min} + \mu^{(2)}\sqrt{k_{\min}k_{\max}}\right)}{\left(\mu^{(1)}k_{\min} + \mu^{(2)}\sqrt{k_{\min}k_{\max}}\right)} \frac{\left(\mu^{(1)}k_{\min} - \mu^{(1)}\sqrt{k_{\min}k_{\max}}\right)}{\left(-\mu^{(2)}k_{\min} - \mu^{(1)}\sqrt{k_{\min}k_{\max}}\right)}. \tag{3.16}$$

To prove Theorem 3.1 several Lemmas are now introduced.

Lemma 3.3 *Under the assumptions*

$$0 < k_{\min} < \widetilde{\alpha} < k_{\max}, \tag{3.17}$$

and if $\widetilde{\alpha}$ is supposed to be known, the function $|\kappa(\widetilde{\alpha},k)|$ defined for $k \in (k_{\min},k_{\max})$, reaches its minimum at the frequency $k^* = \widetilde{\alpha}$.

Proof 3.3 *Substituting $\Theta^{(1)}$ and $\Theta^{(2)}$ given by (3.13) in the expression of the convergence rate (2.9) leads to:*

$$|\kappa(\widetilde{\alpha},k)| = \left|\frac{\mu^{(1)}\mu^{(2)}(-k+\widetilde{\alpha})^2}{(\mu^{(1)}k + \mu^{(2)}\widetilde{\alpha})(\mu^{(2)}k + \mu^{(1)}\widetilde{\alpha})}\right|.$$

It is clear that $|\kappa(\widetilde{\alpha},k)|$ vanishes for the frequency $k^* = \widetilde{\alpha}$. Because the function $|\kappa(\widetilde{\alpha},k)|$ takes positive value only, the frequency k^* is obviously the frequency where the function reaches its minimum.

Lemma 3.4 *Under the assumptions*

$$0 < \mu^{(1)} < \mu^{(2)}, \quad \text{and} \quad 0 < k_{\min} < \widetilde{\alpha} < k_{\max}, \tag{3.18}$$

and if $\widetilde{\alpha}$ is supposed to be known, the function $|\kappa(\widetilde{\alpha}, k)|$ defined for $k \in (k_{\min}, k_{\max})$ reaches its maximum either at the frequency $k^* = k_{\min}$ or at the frequency $k^* = k_{\max}$.

Proof 3.4 *The derivative of the function $|\kappa(\widetilde{\alpha}, k)|$ upon the variable k can be computed as:*

$$\kappa_k(\widetilde{\alpha}, k) = \frac{-\mu^{(1)}\mu^{(2)}(-k+\widetilde{\alpha})\widetilde{\alpha}(\mu^{(1)}+\mu^{(2)})^2(k+\widetilde{\alpha})}{(\mu^{(1)}k+\mu^{(2)}\widetilde{\alpha})^2(\mu^{(2)}k+\mu^{(1)}\widetilde{\alpha})^2}$$

The sign of the function $\kappa_k(\widetilde{\alpha}, k)$ can be analyzed:

$$\begin{cases} \kappa_k(\widetilde{\alpha}, k) < 0, \ \textit{for } k \in (k_{\min}, \widetilde{\alpha}) & (3.19) \\ \kappa_k(\widetilde{\alpha}, k) = 0, \ \textit{for } k = \widetilde{\alpha} & (3.20) \\ \kappa_k(\widetilde{\alpha}, k) > 0, \ \textit{for } k \in (\widetilde{\alpha}, k_{\max}). & (3.21) \end{cases}$$

From the previous analysis, and because $|\kappa(\widetilde{\alpha}, k)|$ is a continuous function, it is clear, that the maximum is obtained at the extremum of the domain of definition, i.e. either at the frequency $k^* = k_{\min}$ or at the frequency $k^* = k_{\max}$.

Proof 3.5 (of Theorem 3.1) *From Lemma 3.4, the maximum of the function $|\kappa(\alpha, k)|$ upon the variable k is obtained either at the frequency $k_{\min}$ or at the frequency $k_{\max}$. In order to find the optimal parameter α^*, solution of the min-max problem, the quantities $|\kappa(\alpha, k_{\min})|$ and $|\kappa(\alpha, k_{\max})|$ are analyzed upon the value taken by the variable α.*

For a given frequency $\widetilde{k}$, the derivative of the function $|\kappa(\alpha, \widetilde{k})|$ upon the variable α can be expressed as:

$$\kappa_\alpha(\alpha, \widetilde{k}) = \frac{\mu^{(1)}\mu^{(2)}(-\widetilde{k}+\alpha)\widetilde{k}\left((\mu^{(1)}+\mu^{(2)})^2\alpha + (\mu^{(1)}+\mu^{(2)})^2\widetilde{k}\right)}{(\mu^{(1)}\widetilde{k}+\mu^{(2)}\alpha)^2(\mu^{(2)}\widetilde{k}+\mu^{(1)}\alpha)^2}.$$

The sign of this function can be analyzed and leads to:

$$\begin{cases} \kappa_\alpha(\alpha, \widetilde{k}) < 0, \ \textit{for } \alpha \in (0, \widetilde{k}) & (3.22) \\ \kappa_\alpha(\alpha, \widetilde{k}) = 0, \ \textit{for } \alpha = \widetilde{k} & (3.23) \\ \kappa_\alpha(\alpha, \widetilde{k}) > 0, \ \textit{for } \alpha \in (\widetilde{k}, +\infty). & (3.24) \end{cases}$$

From the previous analysis and the assumption $k_{\min} < \alpha$, it follows that the function $|\kappa(\alpha, k_{\min})|$ increases for $\alpha \in (k_{\min}, k_{\max})$, from 0 up to $|\kappa(k_{\max}, k_{\min})|$. The same argument with $\alpha < k_{\max}$ implies that the function $|\kappa(\alpha, k_{\max})|$ decreases for $\alpha \in (k_{\min}, k_{\max})$, from $|\kappa(k_{\min}, k_{\max})|$ down to 0. Their respective graphs obviously intersect when $|\kappa(\alpha^*, k_{\min})| = |\kappa(\alpha^*, k_{\max})|$; this leads to the value $\alpha^* = \sqrt{k_{\min} k_{\max}}$. For this value of the parameter α, the quantity

$$\max\left(|\kappa(\alpha, k_{\min})|, |\kappa(\alpha, k_{\max}|)\right)$$

is minimum, which means that α^* is solution of the min-max problem (3.3).

As a summary, the maximum of the function $|\kappa(\alpha, k)|$ is reached at one of the following frequency: $k_{\min}$ or $k_{\max}$. The value of the maximum of the function $|\kappa(\alpha, k)|$ is then given by:

$$\begin{cases} |\kappa(\alpha, k_{\max})| = \left| \dfrac{\mu^{(2)} k_{\max} - \alpha}{\mu^{(1)} k_{\max} + \alpha} \dfrac{\mu^{(1)} k_{\max} - \alpha}{\mu^{(2)} k_{\max} + \alpha} \right|, & \text{if } \alpha < \sqrt{k_{\min} k_{\max}} \quad (3.25) \\ |\kappa(\alpha, k_{\max})| = |\kappa(\alpha, k_{\min})|, & \text{if } \alpha = \sqrt{k_{\min} k_{\max}} \quad (3.26) \\ |\kappa(\alpha, k_{\min})| = \left| \dfrac{\mu^{(2)} k_{\min} - \alpha}{\mu^{(1)} k_{\min} + \alpha} \dfrac{\mu^{(1)} k_{\min} - \alpha}{\mu^{(2)} k_{\min} + \alpha} \right|, & \text{if } \alpha > \sqrt{k_{\min} k_{\max}}. \quad (3.27) \end{cases}$$

Substituting in the expression of the convergence rate, the coefficient α by its optimal value $\alpha^* = \sqrt{k_{\min} k_{\max}}$ gives:

$$\frac{(-\mu^{(2)} k_{\min} + \mu^{(2)} \sqrt{k_{\min} k_{\max}})(\mu^{(1)} k_{\min} - \mu^{(1)} \sqrt{k_{\min} k_{\max}})}{(\mu^{(1)} k_{\min} + \mu^{(2)} \sqrt{k_{\min} k_{\max}})(-\mu^{(2)} k_{\min} - \mu^{(1)} \sqrt{k_{\min} k_{\max}})}, \quad (3.28)$$

which leads to the stated result.

Remark 3.2 *It should be noticed that preliminary works [14] have used this optimal parameter, as derived from the analysis of fluid flow in homogeneous media [23] in the particular case of saturated porous media. Here, the originality leads in the demonstration of this optimal parameter directly from the initial equation in heterogeneous media.*

Theorem 3.2 *The asymptotic convergence rate (2.9) of the non-overlapping Schwarz method with optimized Robin interface conditions discretized with mesh parameter h is given by*

$$\kappa = 1 - \left(2 - \frac{\mu^{(1)}}{\mu^{(2)}} - \frac{\mu^{(2)}}{\mu^{(1)}}\right) \sqrt{k_{\min}} \sqrt{\frac{h}{\pi}} + O(h). \quad (3.29)$$

Proof 3.6 *Since on a numerical grid with grid spacing h the highest frequencies representable are of the order $k_{\max} = \pi/h$, the computation of the expansion in h of the optimized convergence rate $|\kappa(\alpha^*, k)|$ given in (3.28) for $k_{\max} = \pi/h$, leads to the stated result.*

Theorem 3.3 *Under the assumption*

$$0 < \mu^{(1)} \ll \mu^{(2)},$$

the non-overlapping Schwarz method with optimized Robin interface conditions chosen according to (3.15) has an asymptotic convergence rate:

$$\kappa = \frac{(-k_{\min} + \sqrt{k_{\min} k_{\max}})^2}{k_{\min}\sqrt{k_{\min} k_{\max}}} \ \frac{\mu^{(1)}}{\mu^{(2)}} + O\left(\frac{{\mu^{(1)}}^2}{{\mu^{(2)}}^2}\right). \tag{3.30}$$

Proof 3.7 *The expansion in h of the optimized convergence rate $|\kappa(\alpha^*, k)|$ given in (3.28) when $\mu^{(2)}$ tends to infinite, leads to the stated result.*

Remark 3.3 *The previous Theorem implies that increasing the heterogeneity between the sub-domains, decreases the convergence rate of the Schwarz algorithm if the mesh parameter remains fixed! This is confirmed by the numerical experiments. If we refine the mesh together with $\frac{\mu^{(1)}}{\mu^{(2)}} \to 0$, we deduce from Theorem 3.2 that the convergence rate remains about constant if h scales like $(\frac{\mu^{(1)}}{\mu^{(2)}})^2$.*

Figure 4 shows the convergence rate obtained for a model problem on the unit square with two sub-domains for $\mu^{(1)} = 1$, $\mu^{(2)} = 10^2$ and $h = 1/400$. Figure 5 shows the maximum of the convergence rate upon the parameter α to be optimized.

The optimal parameter was found to be $\alpha^* = 35.2211$ which gives an overall convergence rate $\kappa^* = 0.2484$. Figure 6 shows the optimized convergence rate associated to this optimal parameter. The average optimized convergence rate described in this sub-section is lower than the optimized convergence rate described in the previous sub-section. Even though only one parameter is used to determine this optimized coefficient, thanks to the fact that the heterogeneity of the media has been taken into account in the local approximations. This makes this optimization procedure more suitable for highly heterogeneous media.

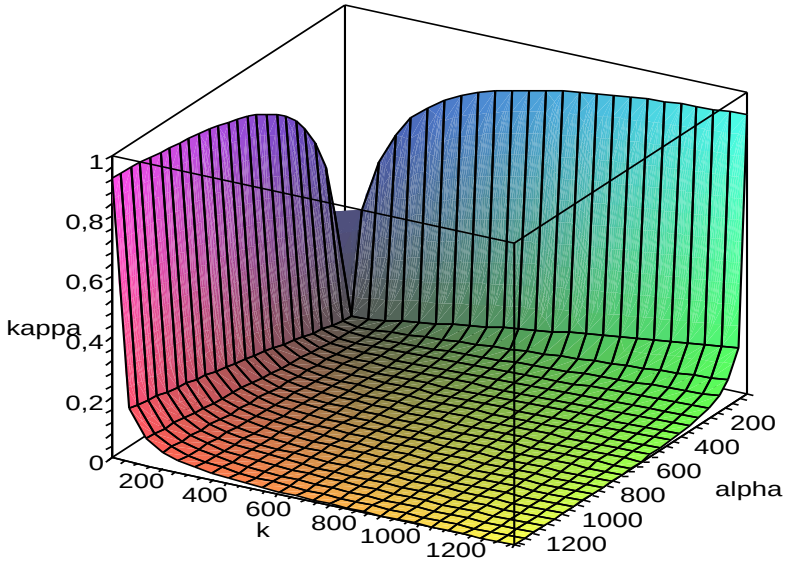

Figure 4: Convergence rate upon the frequency and the parameter to be optimized for $\Theta^{(1)} = \mu^{(2)}\alpha$ and $\Theta^{(2)} = -\mu^{(1)}\alpha$. ($h = 1/400$, $\mu^{(1)} = 1$, $\mu^{(2)} = 10^2$).

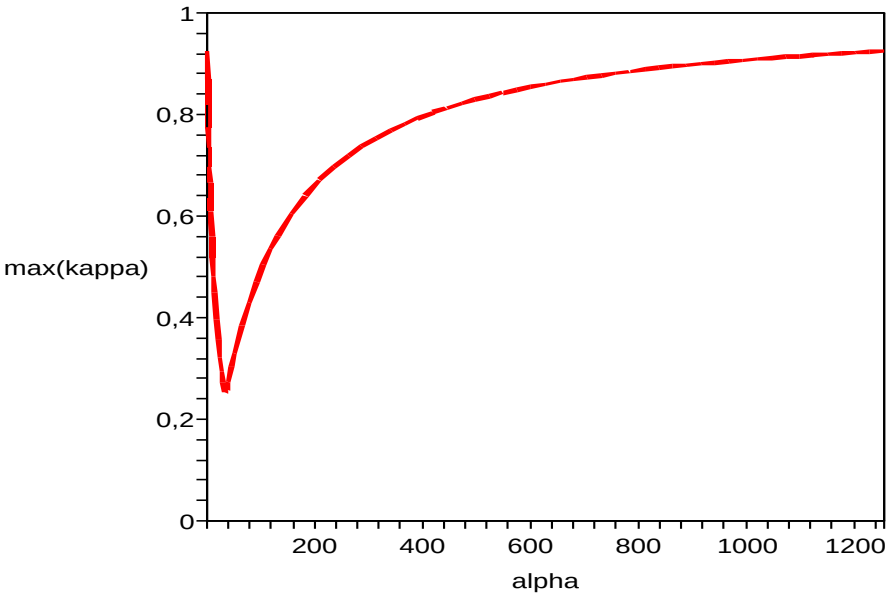

Figure 5: Maximum of the convergence rate upon the parameter to be optimized for $\Theta^{(1)} = \mu^{(2)}\alpha$ and $\Theta^{(2)} = -\mu^{(1)}\alpha$. ($h = 1/400$, $\mu^{(1)} = 1$, $\mu^{(2)} = 10^2$).

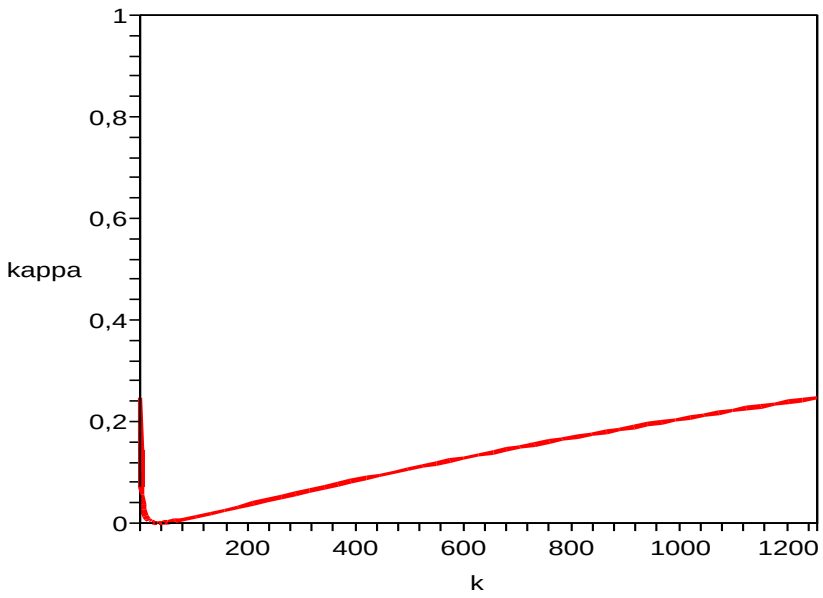

Figure 6: Optimized convergence rate upon the frequency for $\Theta^{(1)} = \mu^{(2)}\alpha^*$, $\Theta^{(2)} = -\mu^{(1)}\alpha^*$. ($h = 1/400$, $\mu^{(1)} = 1$, $\mu^{(2)} = 10^2$).

3.3 Two Parameters Based Robin Interface Conditions

Due to the heterogeneity of the media, it may be interesting to consider even more different local approximations of the optimal operators on each side of the interface. The following approximations are now considered, based on a generalization of (3.13) that process already the good scaling:

$$\Theta^{(1)} = \mu^{(2)}\alpha, \quad \Theta^{(2)} = -\mu^{(1)}\beta \tag{3.31}$$

with $\alpha \in \mathbb{R}^+$ and $\beta \in \mathbb{R}^+$. Substituting $\Theta^{(1)}$ and $\Theta^{(2)}$ in the expression of the convergence rate (2.9) leads to the optimization problem:

$$\min_{\alpha,\beta\in\mathbb{R}^+\times\mathbb{R}^+} \left(\max_{k\in(k_{\min},k_{\max})} \left| \frac{\mu^{(2)}|k| - \mu^{(2)}\alpha}{\mu^{(1)}|k| + \mu^{(2)}\alpha} \; \frac{\mu^{(1)}|k| - \mu^{(1)}\beta}{\mu^{(2)}|k| + \mu^{(1)}\beta} \right| \right).$$

Using two parameters α and β for the optimization problem complicates significantly the analysis. The determination of the analytical expression of the optimal parameters is still under current investigation, and here these parameters will be obtained trough numerical optimization.

As an example we consider the parameters $\mu^{(1)} = 1$, $\mu^{(2)} = 10^2$, and $h = 1/400$. The maximum value of the function $|\kappa(\alpha, \beta, k)|$ over the considered frequencies $(k_{\min}, k_{\max})$ is represented upon the parameters α and β in the Figure 7.

The optimal parameters were found to be $\alpha^* = 657.2791$ and $\beta^* = 1.887$ which gives an overall convergence rate $\kappa^* = 0.008947$. It is interesting to notice that the scaling is even increased with the relation (3.31), which was not obvious. Figure 8 shows the optimized convergence rate associated with these optimal parameters. It is important to notice the scale of the vertical axis which differs from the previous Figures. The optimized convergence rate is indeed much lower than the optimized convergence rate obtained in the previous sub-sections.

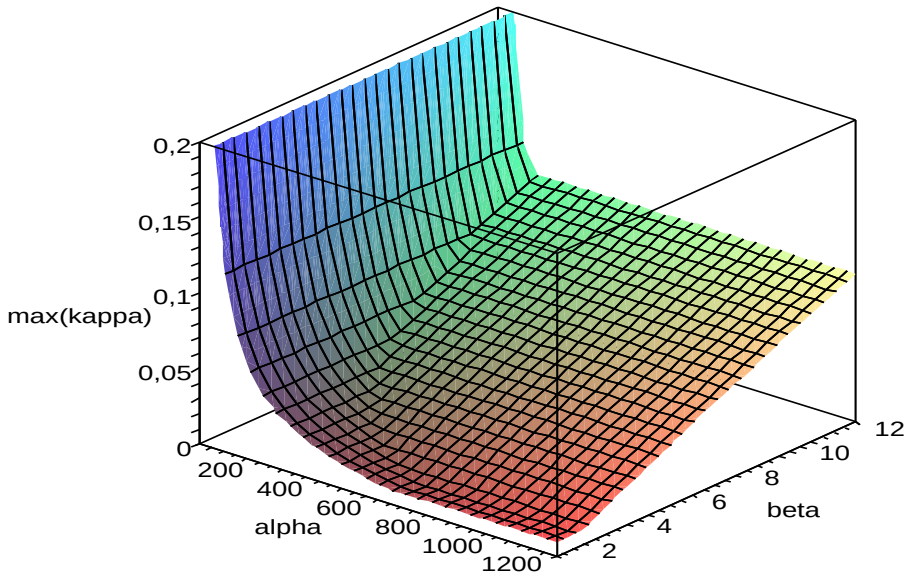

Figure 7: Maximum of the convergence rate upon the parameter to be optimized for $\Theta^{(1)} = \mu^{(2)}\alpha$ and $\Theta^{(2)} = -\mu^{(1)}\beta$. ($h = 1/400$, $\mu^{(1)} = 1$, $\mu^{(2)} = 10^2$).

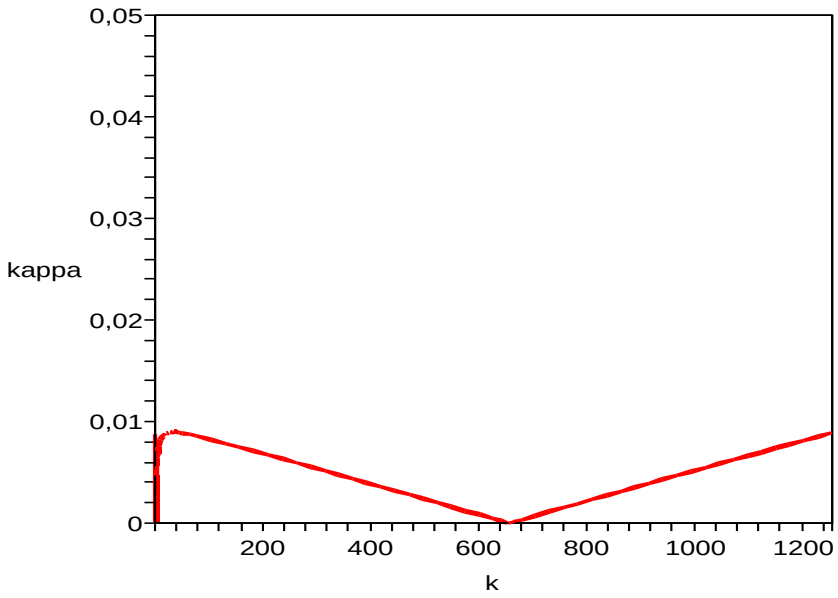

Figure 8: Optimized convergence rate upon the frequency for $\Theta^{(1)} = \mu^{(2)}\alpha^*$ and $\Theta^{(2)} = -\mu^{(1)}\beta^*$. ($h = 1/400$, $\mu^{(1)} = 1$, $\mu^{(2)} = 10^2$).

4 System Construction

The global domain Ω is meshed and partitioned into two non-overlapping sub-domains $\Omega^{(1)}$ and $\Omega^{(2)}$ with an interface $\Gamma^{(12)} = \Gamma^{(21)} = \Omega^{(1)} \cap \Omega^{(2)}$. Let $K^{(s)}$, and $b^{(s)}$ denote respectively the stiffness matrix, and the right hand-side vector associated with the sub-domain $\Omega^{(s)}$, $s = 1, 2$, and let $u^{(s)}$ denotes the restriction to $\Omega^{(s)}$ of the solution in the sub-domain. The vector $u^{(s)}$ is partitioned into two components:

$$u^{(s)} = \begin{pmatrix} u_i^{(s)} \\ u_p^{(s)} \end{pmatrix} \tag{4.1}$$

where the subscripts i and p designate internal and interface boundary unknowns, respectively. With these notations the local stiffness matrix and right hand side can be written:

$$K^{(s)} = \begin{pmatrix} K_{ii}^{(s)} & K_{ip}^{(s)} \\ K_{pi}^{(s)} & K_{pp}^{(s)} \end{pmatrix} \quad , \quad b^{(s)} = \begin{pmatrix} b_i^{(s)} \\ b_p^{(s)} \end{pmatrix}.$$

As explained in [28], the discretization of the Schwarz algorithm with 'absorbing' interface condition leads to the following hybrid problems

$$\begin{pmatrix} K_{ii}^{(1)} & K_{ip}^{(1)} \\ K_{pi}^{(1)} & K_{pp}^{(1)} + A_{pp}^{(1)} \end{pmatrix} \begin{pmatrix} u_i^{(1)} \\ u_p^{(1)} \end{pmatrix} = \begin{pmatrix} b_i^{(1)} \\ b_p^{(1)} + \lambda^{(1)} \end{pmatrix} \tag{4.2}$$

$$\begin{pmatrix} K_{ii}^{(2)} & K_{ip}^{(2)} \\ K_{pi}^{(2)} & K_{pp}^{(2)} + A_{pp}^{(2)} \end{pmatrix} \begin{pmatrix} u_i^{(2)} \\ u_p^{(2)} \end{pmatrix} = \begin{pmatrix} b_i^{(2)} \\ b_p^{(2)} + \lambda^{(2)} \end{pmatrix} \tag{4.3}$$

with the continuity constraints:

$$u_p^{(1)} = u_p^{(2)} \tag{4.4}$$

$$\lambda^{(1)} + \lambda^{(2)} = A_{pp}^{(1)} u_p^{(2)} + A_{pp}^{(2)} u_p^{(1)} \tag{4.5}$$

where $A_{pp}^{(s)}$ is the discretization of operator $\mathcal{A}^{(s)}$ for $s = 1, 2$, and where $\lambda^{(s)}$ is an additional unknown introduced to avoid the computation of the normal derivatives [33]. Rather to consider the continuity constraints (4.4) and (4.5) it is more interesting to consider the following:

$$\lambda^{(1)} + \lambda^{(2)} - A_{pp}^{(1)} u_p^{(2)} - A_{pp}^{(2)} u_p^{(2)} = 0 \tag{4.6}$$

$$\lambda^{(1)} + \lambda^{(2)} - A_{pp}^{(1)} u_p^{(1)} - A_{pp}^{(2)} u_p^{(1)} = 0. \tag{4.7}$$

The variables $u_i^{(1)}$ and $u_i^{(2)}$ can be eliminated [28] from the equations (4.2)-(4.3) in favor of $u_p^{(1)}$ and $u_p^{(2)}$. After substitution of $u_p^{(1)}$ and $u_p^{(2)}$ in equations (4.6)-(4.7), the following linear system condensed on the interface is obtained

$$F\lambda = d \tag{4.8}$$

where the matrix F, the vector λ and the right hand side d are

$$\begin{aligned} F &= \begin{pmatrix} I & I - (A_{pp}^{(1)} + A_{pp}^{(2)})[S_{pp}^{(2)} + A_{pp}^{(2)}]^{-1} \\ I - (A_{pp}^{(1)} + A_{pp}^{(2)})[S_{pp}^{(1)} + A_{pp}^{(1)}]^{-1} & I \end{pmatrix} \\ \lambda &= \begin{pmatrix} \lambda^{(1)} \\ \lambda^{(2)} \end{pmatrix}, \quad d = \begin{pmatrix} (A_{pp}^{(1)} + A_{pp}^{(2)})[S_{pp}^{(2)} + A_{pp}^{(2)}]^{-1} c_p^{(1)} \\ (A_{pp}^{(1)} + A_{pp}^{(2)})[S_{pp}^{(1)} + A_{pp}^{(1)}]^{-1} c_p^{(2)} \end{pmatrix} \end{aligned}$$

where the matrix $S_{pp}^{(s)} = K_{pp}^{(s)} - K_{pi}^{(s)}[K_{ii}^{(s)}]^{-1} K_{ip}^{(s)}$ is the so-called Schur complement matrix and the vector $c_p^{(s)} = b_p^{(s)} - K_{pi}^{(s)}[K_{ii}^{(s)}]^{-1} b_i^{(s)}$ is the condensed right hand side in sub-domain $\Omega^{(s)}$, for $s = 1, 2$.

5 Preconditioning With a Coarse Space Correction

5.1 Iterative Method

If λ^0 and $g^0 = F\lambda^0 - d$ are supposed to be known, the iterative solution of the linear system $F\lambda = d$ by the ORTHODIR algorithm [34] consists of updating λ^p with the following procedure:

$$\lambda^{p+1} = \lambda^p + \rho^p w^p \quad \text{with} \quad w^p \in \mathcal{K}_{p+1}(F, g^0)$$

where the Krylov subspace $\mathcal{K}_{p+1}(F, g^0)$ is defined as:

$$\mathcal{K}_{p+1}(F, g^0) = \text{Span}(g^0, Fg^0, F^2 g^0, \ldots, F^{p+1} g^0).$$

The coefficient ρ^p introduced previously is computed such that it minimizes the $F^T F$-norm of the error, i.e.:

$$\begin{aligned} \|\lambda^{p+1} - \lambda\|_{F^T F}^2 &= \|F(\lambda^{p+1} - \lambda)\|_2^2 \\ &= \|F(\lambda^p + \rho^p w^p) - F\lambda\|_2^2 \\ &= \|F(\lambda^p + \rho^p w^p) - d\|_2^2 \end{aligned}$$

where $||.||_2$ denotes the $\mathbb{L}^2$-norm. The iteration $p+1$ of the ORTHODIR algorithm, consists of the following steps:

- update λ^{p+1} and g^{p+1}:

$$\begin{array}{l} \lambda^{p+1} = \lambda^p + \rho^p w^p \\ g^{p+1} = g^p + \rho^p F w^p \end{array} \quad \text{with} \quad \rho^p = \frac{-(g^p \mid Fw^p)}{(Fw^p \mid Fw^p)}.$$

- update w^{p+1} and Fw^{p+1}:

$$\begin{array}{l} w^{p+1} = Fw^p + \sum_{i=1}^{p} \gamma_i^p w^i \\ Fw^{p+1} = F(Fw^p) + \sum_{i=1}^{p} \gamma_i^p (Fw^i) \end{array} \quad \text{with} \quad \gamma_i^p = \frac{-(F(Fw^p) \mid (Fw^i))}{((Fw^i) \mid (Fw^i))}.$$

The brackets around the quantity (Fw^i) are used to show that this quantity has already been computed in the previous steps of the algorithm and do not required an additional matrix-vector product.

5.2 Preconditioned Iterative Method

Let us introduce the subspace $\mathcal{W}$ represented by the rectangular matrix W, where the number of rows is equal to the degrees of freedom on the global interface. In order to accelerate the convergence of the iterative algorithm applied to the linear system $F\lambda = d$, an additional optional constraint is now introduced. The original algorithm is modified in such a way that at each iteration, the descent direction vector $w^p \in \mathcal{K}_{p+1}(F, g^0)$ is replaced by the vector $\tilde{w^p} \in \mathcal{K}_{p+1}(F, g^0) + \mathcal{W}$. The descent direction vector $\tilde{w^p}$ is thus defined like:

$$\tilde{w^p} = w^p + W\mu^p \quad \text{with} \quad \tilde{w^p} \in \mathcal{K}_{p+1}(F, g^0) \oplus \mathrm{Im}(W). \tag{5.1}$$

With this constraint, the coefficients ρ^p and μ^p now minimize the following function:

$$\varphi(\rho^p, \mu^p) = \|F(\lambda^p + \rho^p(w^p + W\mu^p)) - d\|_2^2.$$

The minimum of this function is obtained when the derivative upon the variable μ^p vanishes, i.e.:

$$(FW)^T(F(\lambda^p + \rho^p(w^p + W\mu^p)) - d) = (FW)^T g^{p+1} = 0. \tag{5.2}$$

This equation represents the additional constraint, which is called optional, since the original algorithm converges without it. Since this constraint must be satisfy at each iteration, it comes:

$$(FW)^T g^p = (FW)^T (F\lambda^p - d) = 0, \quad \forall p.$$

Using the previous expression, equation (5.2) can be simplified as:

$$(FW)^T FW\mu^p = -(FW)^T Fw^p. \tag{5.3}$$

Substitution of μ^p from equation (5.3) in (5.1), gives the expression of the new descent direction $\tilde{w^p}$:

$$\tilde{w^p} = Pw^p \quad \text{where} \quad P = I - W((FW)^T FW)^{-1}(FW)^T F.$$

P denotes here a projection operator which ensures that the gradient g^{p+1} computed from Pw^p satisfy the constraint (5.2).

It is important to notice that cancelling out the derivative of φ with respect to the variable ρ^p gives:

$$(F(w^p + W\mu^p))^T (F(\lambda^p + \rho^p(w^p + W\mu^p)) - d) = (F\tilde{w^p})^T (g^p + \rho^p F\tilde{w^p}) = 0$$

$$\Rightarrow \qquad \rho^p = \frac{-(g^p | F\tilde{w^p})}{(F\tilde{w^p} | F\tilde{w^p})}.$$

The expression of ρ^p is the same as the expression obtained in the original ORTHODIR algorithm when the descent direction vector w^p is simply replaced by $\tilde{w^p}$. If the initial solution is such as it satisfy the constraint (5.2), i.e. $(FW)^T g^0 = 0$, the modified ORTHODIR algorithm is similar to the original ORTHODIR algorithm and only the construction of the descent direction vectors differs.

The modified ORTHODIR algorithm consists in determining at the initialization procedure an initial solution of the form $\tilde{\lambda}^0 = \lambda^0 + W\alpha$, such as:

$$(FW)^T (F(\lambda^0 + W\alpha) - d) = 0 \qquad \Rightarrow \qquad (FW)^T FW\alpha = -(FW)^T (F\lambda^0 - d).$$

The solution of this problem allows to compute $\tilde{\lambda}^0$ as:

$$\tilde{\lambda}^0 = \lambda^0 - W((FW)^T FW)^{-1}(FW)^T(F\lambda^0 - d).$$

The initial gradient g^0 is thus equal to:

$$g^0 = F\tilde{\lambda}^0 - d$$

and the initial descent direction is equal to:

$$w^0 = Pg^0.$$

This initialization ensures that at the first iteration, the value of λ^1 computed from w^0, satisfies the constraint (5.2).

The iteration $p+1$ of the modified ORTHODIR algorithm is similar to the original ORTHODIR algorithm, where the quantities Fw^p are projected before updating the descent direction vectors w^{p+1} and Fw^{p+1}. The different steps are now reminded:

- update λ^{p+1} and g^{p+1}:

$$\begin{array}{l} \lambda^{p+1} = \lambda^p + \rho^p w^p \\ g^{p+1} = g^p + \rho^p F w^p \end{array} \quad \text{with} \quad \rho^p = \frac{-(g^p \mid Fw^p)}{(Fw^p \mid Fw^p)}$$

- update w^{p+1} and Fw^{p+1}:

$$\begin{array}{l} w^{p+1} = PFw^p + \sum_{i=1}^p \gamma_i^p w^i \\ Fw^{p+1} = F(PFw^p) + \sum_{i=1}^p \gamma_i^p (Fw^i) \end{array} \quad \text{with} \quad \gamma_i^p = \frac{-(F(PFw^p) \mid (Fw^i))}{((Fw^i) \mid (Fw^i))}$$

where the brackets around the quantity (Fw^i) and (PFw^p) are used to show that these quantities have been computed in the previous steps of the algorithm.

The computation of the projection of Fw^p consists of solving the additional following problem:

$$(FW)^T FW\mu^p = -(FW)^T Fw^p. \tag{5.4}$$

The computational cost of this operation depends on the number of columns of the matrix W. This number is usually chosen small compared to the dimension of the matrix F. So the matrix $(FW)^T FW$ can be assembled and the solution of the problem (5.4) can be obtained with a direct method. If the number of columns of the matrix W is proportional to the number of sub-domains, the solution at each iteration of the additional problem (5.4) induces a global communication of the information between the sub-domains. Furthermore, the associated cost is very low. In such a case, the procedure is called 'coarse grid', since each sub-domain is assimilated to an element. The space $\mathcal{W}$ is called 'coarse space', and equation (5.1) corresponds to a 'coarse space correction'.

5.3 Constructing the Coarse Basis

The efficiency of the multilevel iterative method is mainly based on the choice of the matrix W or similarly on the choice of the space $\mathcal{W}$. A possibility is to consider the space $\mathcal{W}$ spanned with the restriction on each interface of 'particular' functions defined in each sub-domain, such that $\mathcal{W} = \mathcal{W}^{(1)} \oplus \ldots \oplus \mathcal{W}^{(N_s)}$, for $s = 1..N_s$. Such a choice will reduce significantly the computational cost of the projector P since the interfaces $\Gamma^{(sq)}$ and $\Gamma^{(qs)}$ appears twice between the sub-domains $\Omega^{(s)}$ and $\Omega^{(q)}$.

The rigid body motions introduced in [35] have mainly two goals. The first one is to determine the pseudo-inverse of the sub-domains matrices, and the second one is to accelerate the convergence of the iterative algorithm by using a global communication procedure. Because of the 'absorbing' interface conditions considered in this paper, the rigid body motions are no longer mandatory to ensure the well-posedness of the sub-domains matrices. But choosing as a coarse space basis the rigid body motions of the sub-domains matrices without the 'absorbing' interface conditions (2.2)-(2.4) may be a good idea.

The approach considered in this paper consists of choosing in each sub-domain $\Omega^{(s)}$ a space $\mathcal{W}^{(s)}$ spanned with the restriction on each interface $\Gamma^{(sq)}$ of the rigid body motions $\mathcal{N}^{(s)}$ defined in this sub-domain. Such a choice corresponds to $\mathcal{W}^{(s)} = \bigoplus_{q \neq s} \mathcal{N}^{(s)}_{|\Gamma^{(sq)}}$ and imply that the associated matrix $W^{(s)}$ is diagonal per block. Each block is associated with an interface $\Gamma^{(sq)}$ between the sub-domain $\Omega^{(s)}$ and $\Omega^{(q)}$. These basis functions are multiplied by the matrix $A^{(s)}_{pp}$ in order to keep the homogeneity with the Lagrange multipliers.

6 Numerical Results

Three sets of numerical experiments are now analyzed. The first set corresponds to the model problem analyzed in this paper and the results obtained illustrate the analysis and confirm the asymptotic convergence results. The second set consists in analyzing the robustness of the method when more than two sub-domains are considered, and when cross-points appears, i.e. points where more than two sub-domains intersect. The third set shows the efficiency of the method when applying a coarse space correction.

A two dimensional cavity on the unit square Ω with Dirichlet conditions on the left and with Neuman conditions on the top, on the bottom and on the right is considered. The problem to solve is thus:

$$\begin{cases} (-\nabla \cdot (\mu \nabla) u) = 0, \quad \forall (x,y) \in]0,1[\times]0,1[\\ u(x,y) = u_0(x,y), \quad x = 0, y \in [0,1] \\ \partial_x u(x,y) = \partial_x u_0(x,y), \quad x = 1, y \in [0,1] \\ \partial_y u(x,y) = \partial_y u_0(x,y), \quad x \in [0,1], y = 0,1 \end{cases}$$

where $u_0(x,y) = 16((2x-1)^2 - (2y-1)^2)$. In the case of homogeneous media of density $\mu = 1$, the solution of this problem is equal to $u_0(x,y)$ and the result is shown Figure 9. An uniform rectangular mesh is used for the discretization, and the unit square is decomposed into two sub-domains of equal size, as shown in the Figure 10. Two analysis are now presented. The first analysis considers the parameters $\mu^{(1)} = 1$ and $\mu^{(2)} = 10^2$. Table 1 shows the number of iterations upon the mesh parameter h for optimized Robin interface conditions involving respectively one (OO1p), one and half (OO1.5p), and two (OO2p) optimal parameters. As expected, the iterative Schwarz algorithm requires

Mesh size h	Schwarz method with Optimized 1p	Schwarz method with Optimized 1.5p	Schwarz method with Optimized 2p
1/50	44	16	8
1/100	56	18	8
1/200	64	20	8
1/400	67	22	8

Table 1: Number of iterations for different interface conditions and different mesh parameter. ($N_s = 2$, $\mu^{(1)} = 1$, $\mu^{(2)} = 10^2$).

more iterations when equipped with the OO1p interface condition than with

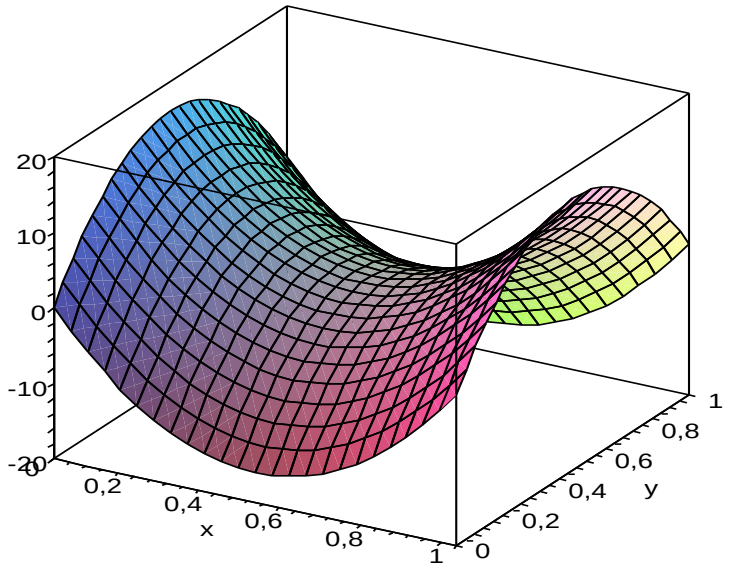

Figure 9: Exact solution of the model problem. ($h = 1/400$, $\mu^{(1)} = \mu^{(2)} = 1$).

the OO1.5p, or the OO2p. It is important to notice the fantastic improvement of the OO1.5p and the OO2p interface condition over the OO1p interface condition. This can be explained by the fact that keeping the property of the heterogeneity between the sub-domains on the interface, leads to good approximation of the Steklov-Poincaré operator. This property of the OO1.5 and OO2p interface condition will be confirmed in the Table 2.

The second analysis considers different parameters $\mu^{(1)}$ and $\mu^{(2)}$. The Schwarz algorithm with OO1p interface conditions leads to more iterations when the heterogeneity between the sub-domains increases. Opposite when equipped with the OO1.5p and the OO2p interface conditions, the algorithm requires less and less iterations. In other words, the strongest is the heterogeneity, the fewer iterations are required to solve the problem.

The robustness of the Schwarz algorithm equipped with the OO1p, OO1.5p, and OO2p interface conditions is now analyzed when more than two sub-domains are involved in the mesh partition. Figure 11 shows the partition of the domain Ω in one spatial direction. Table 3 shows the number of iterations for different interface conditions and different number of sub-domains. Since no coarse space correction are used at the moment, increasing the number of

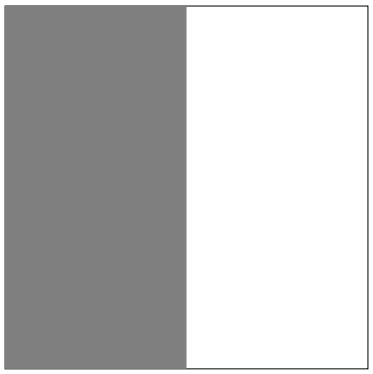

Figure 10: Mesh partition into two sub-domains.

Heterogeneity ratio $\mu^{(2)}/\mu^{(1)}$	Schwarz method with Optimized 1p	Schwarz method with Optimized 1.5p	Schwarz method with Optimized 2p
10	48	32	12
10^2	56	18	8
10^3	71	10	3
10^4	80	8	6

Table 2: Number of iterations for different interface conditions and different ratio of heterogeneity between the media. ($N_s = 2$, $h = 1/100$).

sub-domains increases the number of iterations. This property is confirmed in the Table 4 for a partition of the domain Ω in two spatial directions as shown in the Figure 12. It is important to notice the existence of several cross-points in the mesh partition. Anyway, even with such configuration, the algorithm converges with all the proposed interface conditions. The OO1.5p and the OO2p interface conditions reduces the number of iteration by a factor four in comparison to the OO1p interface conditions.

Finally a coarse space correction is applied to the linear system condensed on the interface. The results in the Table 5 show that a scalability of the Schwarz algorithm with the OO1.5p and the OO2p interface conditions can be obtained. Unfortunately, such a coarse space correction does not lead to good results when cross-points exist, an issue under current investigation.

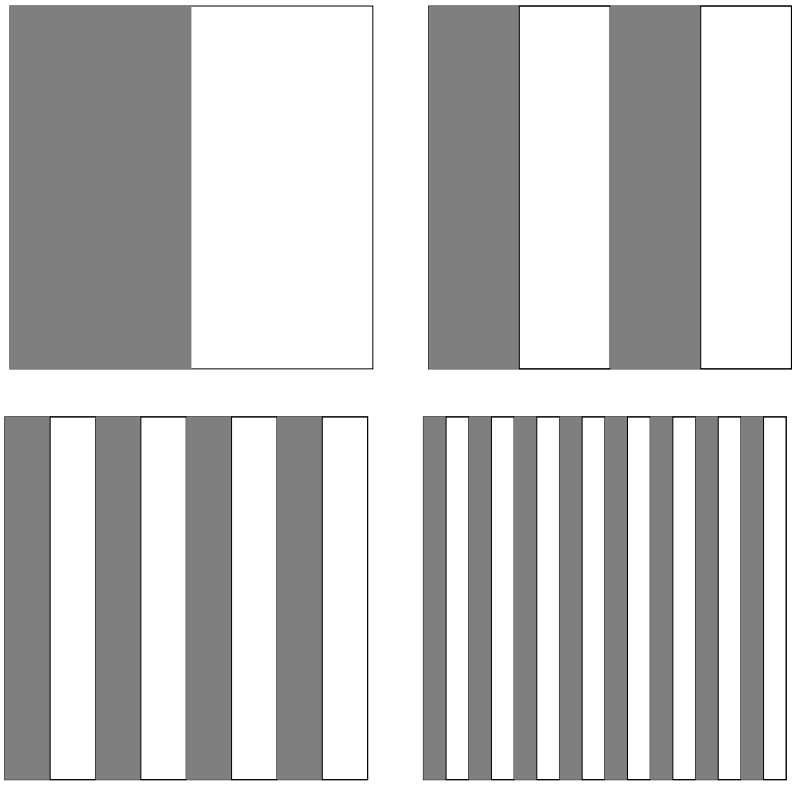

Figure 11: Mesh partition in one spatial direction.

7 Conclusion

In this paper an original variant of the Schwarz domain decomposition method is introduced for heterogeneous media. This method uses new optimized 'absorbing' interface conditions specially designed for highly heterogeneous media. Three techniques of optimization to design these interface conditions are proposed. These techniques are based on the optimization of one, one and half, or two parameters respectively. Two of these techniques are designed to keep the property of the heterogeneity of the media between the sub-domains on the interface.

After the theoretical analysis of the proposed optimization problems, several numerical experiments illustrate the robust convergence properties of the algorithm for highly heterogeneous media. Beyond the proposed techniques,

Number of sub-domains N_s	Schwarz method with Optimized 1p	Schwarz method with Optimized 1.5p	Schwarz method with Optimized 2p
2	56	18	8
4	68	20	12
8	76	22	16
12	82	26	22
16	86	32	27

Table 3: Number of iterations for different interface conditions and different number of sub-domains issue from a mesh partition in one spatial direction. ($h = 1/100$, $\mu^{(2s+1)} = 1$, $\mu^{(2s)} = 10^2$, $s = 0..8$).

Number of sub-domains N_s	Schwarz method with Optimized 1p	Schwarz method with Optimized 1.5p	Schwarz method with Optimized 2p
4	60	16	10
9	75	21	14
16	116	36	26
25	126	36	32

Table 4: Number of iterations for different interface conditions and different number of sub-domains issue from a mesh partition in two spatial directions. ($h = 1/100$, $\mu^{(2s+1)} = 1$, $\mu^{(2s)} = 10^2$, $s = 0..8$).

two of them give outstanding results, by decreasing the number of iterations when increasing the heterogeneity of the media between the sub-domains. This property makes these techniques very convenient for application to ill-conditioned problems. Even though the theoretical analysis has been performed on two half space, all these techniques perform well when the mesh partitioning involves several sub-domains and cross points between these sub-domains. All these results make the Schwarz algorithm equipped with the proposed interface conditions a very promising solver to solve highly heterogeneous media. An additional coarse space correction allows to obtain a scalability in the case of a mesh partition in one spatial direction. Further improvements to build efficient coarse space basis in the case of general mesh partition should be analyzed in the future.

References

[1] H.A. Schwarz. Über einen Grenzübergang durch alternierendes Verfahren. *Vierteljahrsschrift der Naturforschenden Gesellschaft in Zürich*, 15:272–

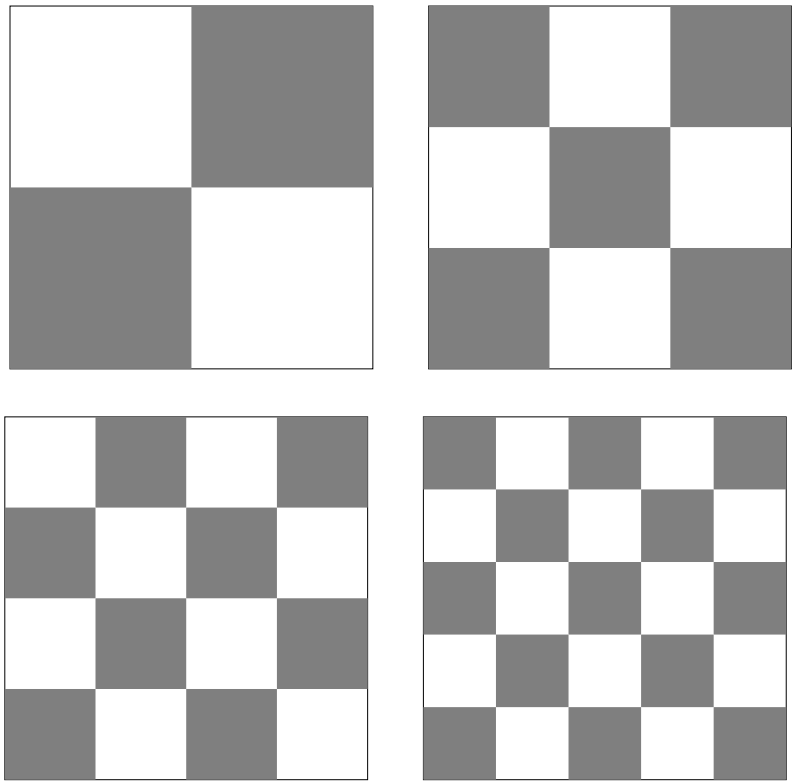

Figure 12: Mesh partition in two spatial directions.

286, May 1870.

[2] H.A. Schwarz. *Gesammelte Mathematische Abhandlungen*, volume 2, pages 133–143. Springer, Berlin, 1890. First published in Vierteljahrsschrift der Naturforschenden Gesellschaft in Zürich, volume 15, 1870, pp. 272–286.

[3] P.-L. Lions. On the Schwarz alternating method. I. In Roland Glowinski, Gene H. Golub, Gérard A. Meurant, and Jacques Périaux, editors, *First International Symposium on Domain Decomposition Methods for Partial Differential Equations*, pages 1–42, Philadelphia, PA, 1988. SIAM.

[4] P.-L. Lions. On the Schwarz alternating method. II. In Tony Chan, Roland Glowinski, Jacques Périaux, and Olof Widlund, editors, *Domain*

Number of sub-domains N_s	Without a coarse space correction			With a coarse space correction		
	Optimized 1p	Optimized 1.5p	Optimized 2p	Optimized 1p	Optimized 1.5p	Optimized 2p
4	68	20	12	59	14	8
8	76	22	16	62	14	8
12	82	26	22	64	16	10
16	86	32	27	65	16	10

Table 5: Number of iterations for different interface conditions and different number of sub-domains issue from a mesh partition in one spatial direction. ($h = 1/100$, $\mu^{(2s+1)} = 1$, $\mu^{(2s)} = 10^2$, $s = 0..8$).

Decomposition Methods, pages 47–70, Philadelphia, PA, 1989. SIAM.

[5] P.-L. Lions. On the Schwarz alternating method. III: a variant for nonoverlapping subdomains. In Tony F. Chan, Roland Glowinski, Jacques Périaux, and Olof Widlund, editors, *Third International Symposium on Domain Decomposition Methods for Partial Differential Equations, held in Houston, Texas, March 20-22, 1989*, Philadelphia, PA, 1990. SIAM.

[6] P.E. Bjørstad and O.B. Widlund. To overlap or not to overlap: A note on a domain decomposition method for elliptic problems. *SIAM J. Sci. Stat. Comput.*, 10(5):1053–1061, 1989.

[7] A. Quarteroni and A. Valli. *Domain Decomposition Methods for Partial Differential Equations*. Oxford Science Publications, 1999.

[8] A. Toselli and O. Widlund. *Domain Decomposition Methods - Algorithms and Theory*, volume 34 of *Springer Series in Computational Mathematics*. Springer, 2004.

[9] M.J. Gander, L. Halpern, and F. Nataf. Optimized Schwarz methods. In Tony Chan, Takashi Kako, Hideo Kawarada, and Olivier Pironneau, editors, *Twelfth International Conference on Domain Decomposition Methods, Chiba, Japan*, pages 15–28, Bergen, 2001. Domain Decomposition Press.

[10] L. Tourrette and L. Halpern, editors. *Absorbing boundaries and layers, domain decomposition methods, application to large scale computations*. Novascience, 2001.

[11] F. Collino, S. Ghanemi, and P. Joly. Domain decomposition methods for harmonic wave propagation : a general presentation. *Comput. Methods Appl. Mech. Engrg*, (2-4):171–211, 2000.

[12] M. Garbey and D. Tromeur-Dervout. Aitken-Schwarz method on Cartesian grids. In N. Debit, M. Garbey, R. Hoppe, J. Périaux, and D. Keyes, editors, *Proc. Int. Conf. on Domain Decomposition Methods DD13*, pages 53–65. CIMNE, 2002.

[13] M. Garbey and D. Tromeur-Dervout. Parallel algorithms with local Fourier basis. *J. Comput. Phys.*, 173(2):575–599, 2001.

[14] M. Garbey and D. Tromeur-Dervout. On some Aitken like acceleration of the Schwarz method. *Int. J. for Numerical Methods in Fluids*, 2002 (in press).

[15] S.C. Brenner. A two-level Schwarz preconditioner for nonconforming plate elements. *Numer. Math.*, 72(4):419–447, 1996.

[16] M. Brezina and P. Vanek. A black-box iterative solvers based on a two-level Schwarz method. *Computing*, 63:233–363, 1999.

[17] X.-C. Cai. An optimal two-level overlapping domain decomposition method for elliptic problems in two and three dimensions. *SIAM J. Sci. Comp.*, 14:239–247, January 1993.

[18] L. Carvalho, L. Giraud, and G. Meurant. Local preconditioners for two-level non-overlapping domain decomposition methods. Technical report tr/pa/99/38, CERFACS, Toulouse, France, 1999. Preliminary version of the paper to appear in Numerical Linear Algebra with Applications.

[19] M.V. Sarkis. Two-level Schwarz methods for nonconforming finite elements and discontinuous coefficients. In N. Duane Melson, Thomas A. Manteuffel, and Steve F. McCormick, editors, *Proceedings of the Sixth Copper Mountain Conference on Multigrid Methods, Volume 2*, number 3224, pages 543–566, Hampton VA, 1993. NASA.

[20] C. Farhat, A. Macedo, M. Lesoinne, F.-X. Roux, F. Magoulès, and A. de la Bourdonnaye. Two-level domain decomposition methods with Lagrange multipliers for the fast iterative solution of acoustic scattering problems.

Computer Methods in Applied Mechanics and Engineering, 184(2):213–240, 2000.

[21] P. Goldfeld, L.F. Pavarino, and O.B. Widlund. Balancing Neumann-Neumann preconditioners for mixed approximations of heterogeneous problems in linear elasticity. Technical Report 825, Courant Institute of Mathematical Sciences, Computer Science Department, April 2002.

[22] L. Gerardo Giorda and F. Nataf. Optimized schwarz methods for unsymmetric layered problems with strongly discontinuous and anisotropic coefficients. Technical Report 561, CMAP, CNRS UMR 7641, Ecole Polytechnique, France, 2004. submitted.

[23] L. Saas, I. Faille, F. Nataf, and F. Willien. Finite volume methods for domain decomposition on nonmatching grids with arbitrary interface conditions and highly heterogeneous media. In R. Kornhuber et al, editor, *Domain Decomposition Methods in Science and Engineering*, pages 283–290. Springer-Verlag, Haidelberg, 2004.

[24] M.J. Gander, F. Magoulès, and F. Nataf. Optimized Schwarz methods without overlap for the Helmholtz equation. *SIAM Journal on Scientific Computing*, 24(1):38–60, 2002.

[25] V. Dolean, S. Lanteri, and F. Nataf. Convergence analysis of a Schwarz type domain decomposition method for the solution of the Euler equations. Technical Report 3916, INRIA, aopr 2000.

[26] P. Chevalier and F. Nataf. Symmetrized method with optimized second-order conditions for the Helmholtz equation. In *Domain decomposition methods, 10 (Boulder, CO, 1997)*, pages 400–407. Amer. Math. Soc., Providence, RI, 1998.

[27] F. Magoulès and I. Harari, editors. *Absorbing Boundary Conditions*. Computer Methods in Applied Mechanics and Engineering, 2005 (in press).

[28] F. Magoulès, P. Iványi, and B.H.V. Topping. Non-overlapping Schwarz methods with optimized transmission conditions for the Helmholtz equation. *Computer Methods in Applied Mechanics and Engineering*, 193(45–47):4797–4818, 2004.

[29] B. Després. Domain decomposition method and the Helmholtz problem.II. In *Second International Conference on Mathematical and Numerical Aspects of Wave Propagation (Newark, DE, 1993)*, pages 197–206, Philadelphia, PA, 1993. SIAM.

[30] J. D. Benamou and B. Després. A domain decomposition method for the Helmholtz equation and related optimal control problems. *J. of Comp. Physics*, 136:68–82, 1997.

[31] F. Magoulès, P. Iványi, and B.H.V. Topping. Convergence analysis of Schwarz methods without overlap for the Helmholtz equation. *Computers and Structures*, 82:1835–1847, 2004.

[32] F. Magoulès, F.-X. Roux, and S. Salmon. Optimal discrete transmission conditions for a non-overlapping domain decomposition method for the Helmholtz equation. *SIAM Journal on Scientific Computing*, 25(5):1497–1515, 2004.

[33] F. Magoulès, K. Meerbergen, and J.-P. Coyette. Application of a domain decomposition method with Lagrange multipliers to acoustic problems arising from the automotive industry. *Journal of Computational Acoustics*, 8(3):503–521, 2000.

[34] Y. Saad. *Iterative Methods for Sparse Linear Systems*. PWS Publishing Company, 1996.

[35] C. Farhat and F.-X. Roux. Implicit parallel processing in structural mechanics. In J. Tinsley Oden, editor, *Computational Mechanics Advances*, volume 2 (1), pages 1–124. North-Holland, 1994.